

하이퍼볼릭 평면에서의 지역적 MQ 보간법

박 화 진[†]

요 약

본 논문에서는 하이퍼볼릭 평면에서 임의의 분산 데이터 보간을 지역적으로 제어하는 새로운 방법을 개발하였다. 지역적 제어와 관련된 주제는 상호대화형식의 디자인분야에서 매우 중요하다. 특히 본 논문에서 제안한 방법은 하이퍼볼릭 평면상에서 형성되는 genus-N 객체 모델은 상호대화형식으로 디자인하는데 유효하게 적용될 수 있다. 즉 변화된 데이터가 미치는 영향이 일정한 지역에만 국한되므로 일반 사용자가 genus-N 객체를 상호대화형식으로 디자인하기가 훨씬 편리하다. 따라서, 본 연구는 genus-N 객체를 형성하는데 사용한 하이퍼볼릭 평면에서의 지역적 보간법을 발전시켜 하이퍼볼릭 평면에서의 지역적 보간법개발 및 구현을 목적으로 하고있다. 이는 다음과 같은 주요 과정을 통하여 구현된다. 먼저, 보간 함수를 지역화하기 위하여 하이퍼볼릭 영역을 임의의 삼각형 패치로 세분화하고 각 데이터에 인접한 삼각형 패치들의 모임을 부 영역이라고 정의한다. 각 부 영역에는 가중치 함수가 설정된다. 마지막으로 중첩된 삼각형 영역의 세 개의 가중치를 혼합함으로써 지역적 보간 함수가 완성된다. 그 결과로서, 여러 개의 샘플 데이터 및 함수를 사용하여 지역적MQ 보간법과 비교한다.

A Localized Multiquadric (MQ) Interpolation Method on the Hyperbolic Plane

Hwa-Jin Park[†]

ABSTRACT

A new method for local control of arbitrary scattered data interpolation in the hyperbolic plane is developed in this paper. The issue associated with local control is very critical in the interactive design field. Especially the suggested method in this paper could be effectively applied to the interactive shape modeling of genus-N objects, which are constructed on the hyperbolic plane. Since the effects of the changed data affects only the limited area around itself, it is more convenient for end-users to design a genus-N object interactively. Therefore, by improving the global interpolation on the hyperbolic plane where the genus-N object is constructed, this research is aiming at the development and implementation of the local interpolation on the hyperbolic plane. It is implemented using the following process. First, for localizing the interpolating functions, the hyperbolic domain is tessellated into arbitrary triangle patches and the group of adjacent triangle patches of each data point is defined as a sub-domain. On each sub-domain, a weight function is defined. Last, by blending of three weight functions on the overlapped triangles, local MQ interpolation is completed. Consequently, it is compared with the global MQ interpolation using several sample data and functions.

키워드 : 하이퍼볼릭 평면(hyperbolic plane), 지역보간법(local interpolation method), multiquadric 함수(multiquadric function), 영역 분할(tessellation)

1. Introduction

Many researchers have improved scattered data interpolation methods in Euclidean plane. The problem of scattered data interpolation is to find a real valued multivariate function interpolating a finite set of arbitrary located data points. If we take bivariate functions as examples, they can be defined in terms of input and output as follows :

Input : n data points (p_i, f_i) , $p_i \in R^2$, $i=1, \dots, n$.

Output : continuous function $f: R^2 \rightarrow R$, interpolating the given data points, that is,

$$f(p_i) = f_i, \quad i = 1, \dots, n.$$

Scattered data interpolation and approximation can be applied in many areas including mineral exploration, computer-aided geometric design, image deformation, earth crustal movement and weather analysis. The survey paper [1, 8] by Barnhill described many of these applications and methods for solving the problem. Several bivariate scattered data interpolations have been tested and compared by Franke [6]. Among them tested by Franke that performed well in that

※ 본 연구는 숙명여자대학교 2000년도 교내연구비 지원에 의해 수행되었음.

† 종신회원 : 숙명여자대학교 정보과학부 멀티미디어학전공 교수

논문접수 : 2001년 5월 10일, 심사완료 : 2001년 10월 10일

comparison, Hardy's multiquadric method, the thin-plated splines of Duchon, and the minimum norm network method are included. Despite these well-performed results, there are some negative aspects that they are not local and they are computationally expensive and unstable if the number of data points is big. Hence, the local control of scattered data interpolation is developed using several different approaches. While Shephard first suggested the inverse distance-weighted method, Hardy[9][10] and Duchon[16] developed local multiquadric method and local thin plate method respectively, which are the most widely used methods.

Recently, many researchers have been exploring the applicable area for the hyperbolic plane. Actually the hyperbolic plane is not new to a mathematician, but is a new field for data interpolation and applicable area in the real world. Such application to the sculpture area is done first by Ferguson[3], a mathematician and also an artist. He suggested the method of modeling the 3D object of N genus ($N=1, \dots, n$) over the single patch. Several methods for modeling a genus N object have been improved to enhance the smoothness and the continuity of the objects, since then. Rockwood [4, 14] showed the way of designing a genus N object interactively from the given scattered data on the hyperbolic plane. Radial basis functions over the hyperbolic plane such as multiquadric, thin plate splines are utilized to interpolate the sampled data from the genus N object. But it embeds the inconvenience in modeling, designing, and editing the sculpture, which comes from global property of the function. To eliminate such problems, a new method for enhancing locality to the interpolating function on the hyperbolic plane has been necessary. In this sense, this paper aims at the new scattered data interpolation method providing the local control property on the hyperbolic plane. Since it is implemented on the hyperbolic plane, the new suggested function is working with the hyperbolic distance. For localizing the interpolating functions, the hyperbolic domain is tessellated into arbitrary triangle patches and divided into several sub-domains. A weight function on each region is defined and blended on the overlapping triangles.

This paper is organized as follows. Section 2 describes the preliminary concepts of the hyperbolic geometry including distance, angle, etc. Several methods of local scattered data interpolation on Euclidean plane are explained in section 3. The next section shows a local scattered data interpolation based on hybrid bezier patches on the hyperbolic plane along with the analysis of the results. Finally, conclusion is fol-

lowing in the section 5.

2. Brief Background on Hyperbolic Geometry

A brief summary of hyperbolic geometry is reviewed. The hyperbolic geometry originates from the hyperboloid model. As it is shown in (Figure 2.1), the hyperboloid model of two sheets can be defined by the equation $x_1^2 - x_2^2 - x_3^2 = 1$ in the homogeneous Cartesian coordinates x_1, x_2, x_3 . Taking either sheet from the hyperbola and mapping it using a central projection into the plane $x_1 = 1$ come up with the hyperbolic unit disc whose radius is 1. The hyperboloid model and the hyperbolic disc are shown in (Figure 2.1). A point p on the upper sheet is mapping to p' in the disc, which is represented as the hyperbolic plane H^2 . This induces the hyperbolic geometry on H^2 , a non-Euclidean geometry. More details are available in [12, 13].

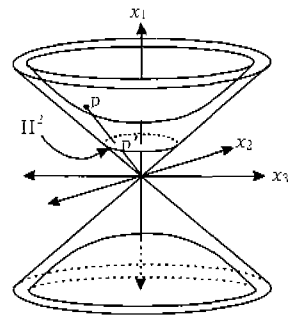


(Figure 2.1) Hyperboloid model

In general, the hyperbolic geometry is different from Euclidean geometry in defining the basic elements. Points in the hyperbolic geometry correspond with points of the unit disc, while lines in the hyperbolic geometry are arcs of circles in the unit disc that are perpendicular to the disc boundary at their endpoints. For an example, arc (PQ) in Euclidean geometry in (Figure 2.2) is considered as the line segment PQ in the hyperbolic geometry. But the diameters of the disc are straight lines. The hyperbolic angle between two hyperbolic lines (arcs) which intersect at a point is the ordinary Euclidean angle between their tangents. Two points can be said to be collinear if and only if they are placed inside the unit disc $D (= H^2)$ and on the circle which meets the boundary at right angles. Two angles in the hyperbolic geometry can be equal if and only if they are equal in Euclidean geometry. Using two points M and N on the boundary of unit disc D which is called 'points at ∞ ', it is possible to define the distance between two points P and

Q in the hyperbolic geometry. Refer to (Figure 2.2). With an assumption that the radius of the disc is 1, the hyperbolic distance d_H between points P and Q is

$$d_H(PQ) = \frac{1}{2} \left| \log_e \frac{d_E(PN)d_E(QM)}{d_E(PM)d_E(QN)} \right|,$$

where P and Q are any two points in the disc and M and N are the points on the boundary of D and on the line (arc) through P and Q where N is closest to P and M is closest to Q . The notation $d_E(PQ)$ means the Euclidean distance between P and Q . The hyperbolic distance between P and Q increases without a limit as P or Q approaches the disc boundary.

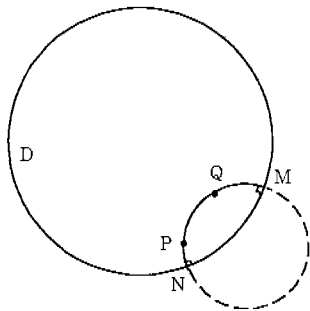


(Figure 2.2) The hyperbolic distance between P and Q

The advantage of the unit disc D is that we can cover the whole plane with a mosaic of almost all regular polygons without overlapping any polygons. We define a *regular tessellation* of the hyperbolic plane as a covering of the entire plane by non-overlapping regular polygons which meet only along complete edges, or at vertices. All polygons in any tessellation must have the same number of sides. A regular tessellation with q regular p -sided polygons (p -gons) meeting at each vertex is denoted by $\{p, q\}$.

Since the sum of angles in a triangle in Euclidean plane is equal to π , we have

$$\pi - \frac{2\pi}{p} = \frac{2\pi}{q},$$

Hence,

$$1 - \frac{2}{p} = \frac{2}{q}.$$

Thus,

$$pq - 2q - 2p = 0$$

$$(p-2)(q-2) = 4$$

We can have three real solutions from this equation, so three regular tessellations in the Euclidean plane, $\{4, 4\}$, $\{6,$

$3\}$, and $\{3, 6\}$, are possible. In the hyperbolic plane, most regular tessellations satisfying

$$(p-2)(q-2) > 4$$

are possible, since the angular sum of any triangle is less than π . Therefore, there are an infinite number of possible regular tessellations on the hyperbolic plane. Detailed explanations on the regular tessellation in the hyperbolic plane can be found in [5].

The marked simple polygon of a genus N object via cuts, called the *fundamental polygon*, can be mapped to the hyperbolic disc and used for regular tessellation by rotation and translation. A translation in H^2 is a fractional linear transformation (Möbius transformation), which reflects itself across an arc. It is given by $f(z) = (az + b)/(cz + d)$, with $ad - bc = 1$. Each translation generates a replication of the polygon, called a period. The regular tessellation with q regular p -sided polygons (p -gons), which meet at each vertex, $\{p, q\}$, forms a group denoted by $\Gamma_{p,q}$. If p is equal to q , Γ_p can be used instead of $\Gamma_{p,q}$.

This research adopted the Poincaré model of the hyperbolic disc in which the edges of the polygon are a special set of $4n$ equivalent length circular arcs and are arranged to form the sides of a regular figure, which is symmetric to the origin. The Poincaré model has a symmetric representation. (Figure 2.3) shows the $\{8, 8\}$ tessellation of the hyperbolic plane.

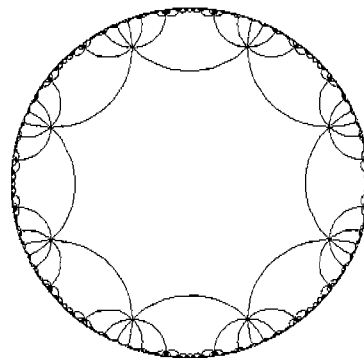


(Figure 2.3) $\{8, 8\}$ tessellation of the hyperbolic plane

3. Localized Scattered Data Interpolation on Euclidean Plane

3.1 Hardy's global multiquadric (MQ) interpolation

MQ interpolation is one of the radial basis functions, in which the term 'radial' is derived from the property that values of the basis function depend only on the distance from

the data point. The coefficients of the basis function is determined by the following form,

$$f(p) = \sum_{i=1}^N \alpha_i B_i(d(p, p_i)) + b_m(p), \quad b_m(p) = \sum_{j=1}^m \beta_j b_j(p),$$

where the basis function $B_i(d(p, p_i))$ are positive radial function, i.e., functions of the distance $d(p, p_i)$ of the point $p = (x, y)$ to the interpolation points $p_i = (x_i, y_i)$ in the parameter space, and $b_j = (x, y)$ is a monomial function of degree at most m . The unknown coefficients α_i and β_j are obtained from the interpolating conditions,

$$f(p_i) = f_i,$$

m side conditions

$$\sum_{i=1}^N \alpha_i b_j(p_i) = 0, \quad j=1, \dots, m$$

and also by solving the resulting system of linear equations.

The MQ method has the following basis function

$$B(r_i) = (r_i^2 + R^2)^{\frac{\mu}{2}}, \quad \mu_i \neq 0,$$

where R is a positive constant. Hardy set the choice of μ to be equal to 1, which corresponds to the upper part of a hyperboloid of rotation. The best choice of r is often the distance between p and p_i ,

$$d(p, p_i) = \sqrt{(x-x_i)^2 + (y-y_i)^2}.$$

With the well-selected parameters r and R , the MQ method generates a good interpolation which is relatively simple to implement, and leads to neat systems of equations for the moderate size of data sets. In addition, the resulting surfaces are C^∞ . More details are in [11].

3.2 Localized multiquadric (MQ) interpolation

The basic technique used in Franke [7] for localizing a global interpolation method uses the following process. First define local domain regions $S_j, j=1, \dots, K$ such that the union of these regions contains the domain of interest for evaluating the final interpolation. Second, define weight functions $W_j(x, y)$ such that

$$\sum_{j=1}^K W_j(x, y) = 1 \text{ for all } (x, y) \text{ inside of } S_j$$

$$W_j(x, y) = 0 \text{ for } (x, y) \text{ outside of } S_j,$$

Third, define local interpolation $Q_j(x, y)$ such that $Q_j(x_i, y_i) = f_i$ for all $i \in \{i : (x_i, y_i) \in S_j\}$. Finally define the localized interpolation to be

$$F(x, y) = \sum_{j=1}^K W_j(x, y) Q_j(x, y)$$

Since the weight functions sum to one, we have that $F(x_i, y_i) = f_i$ for $i=1, \dots, n$.

Therefore the interpolation is local in the sense that $F(x, y)$ only depends on data points (x_i, y_i, f_i) for $i \in J_{(x, y)}$, where $J_{(x, y)} = \{j : (x, y) \in S_j\}$. Since the weight functions have compact support, the localized interpolation can be evaluated as

$$F(x, y) = \sum_{j \in J_{(x, y)}} W_j(x, y) Q_j(x, y)$$

Originally, Franke chose rectangles as the local region by overlapping the domain with a rectangular grid and used standard C^1 piecewise bicubic Hermite basis function as the weight functions. For local interpolation $Q_j(x, y)$, he used thin plate spline (TPS) function. It is quite satisfactory under the assumption that the given sample data are somewhat uniformly distributed in the domain. Foley in [15] suggested a weight function over the overlapping triangular domain using hybrid bezier triangle patches, which is appropriate in the situation that the domain is tessellated into arbitral triangle patches and in the situation that data in some area are very dense and some are sparse. For this research, Foley's method is chosen to tessellate the hyperbolic plane not because of the sampled data but because of the domain. The reason will be explained in section 4.

4. Local Multiquadric(MQ) Interpolating Function on the Hyperbolic Disc.

4.1 Local Multiquadric(MQ) function using hybrid bezier triangle patch on the hyperbolic Disc

The local MQ interpolating function mentioned in section 3 is based on the domain tessellated with the rectangles. However, it is not quite fit to the hyperbolic plane, which is not tessellated with rectangle-based grids, i.e. (4,4). Therefore this research adopts the triangle tessellation, especially, Delaunay triangulation, which avoids long and skinny triangles. Over these triangles, a sub domain S_j is defined as a set of neighboring triangles of vertex V_j . The weighting function on each of subdomain is generated. There are se-

veral weight functions generated over a triangle in Euclidean such as Clough-Tocher triangles, quintic patch in Barnhill and Farin, Foley's hybrid bezier triangle patch. See [2, 15] for more details. The comparisons among them are out of main focus and could be future works. According to [15], however, the weight function over Foley's hybrid bezier triangle domain requires the smallest number of control data points and produces qualitative results. Therefore, the hybrid bezier triangle employing hyperbolic distance on the hyperbolic plane is developed for a smooth interpolation of locality.

First tessellate triangle domain $S_j, j=1, \dots, K$ satisfying whole domain $D=S_1 \cup S_2 \cup \dots \cup S_K$. Each S_j dominates all neighboring triangles of vertex V_j . (Figure 4.1) shows an example of domain S_j .

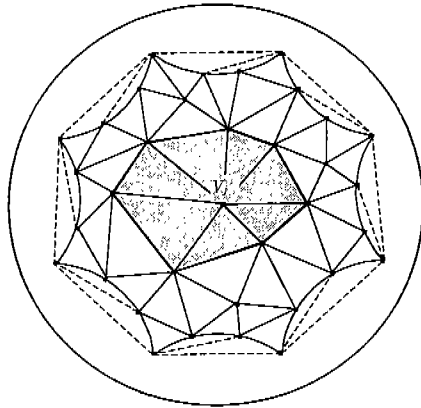


(Figure 4.1) example of domain S_j

Assuming that on each triangle T_{ijk} whose vertices are V_i, V_j , and V_k , we have 12 control points $b_{111}^0, b_{111}^1, b_{111}^2, b_1 = b_{ijk}$, where $|I|=3$ and $|I| \neq (1, 1, 1)$, the hybrid cubic Bezier triangle patch is defined as

$$H(U) = \sum_{|I|=3} b_I B_I(U)$$

where

$$B_I(U) = B_{ijk}(U) = \frac{3!}{i!j!k!} u_0^i u_1^j u_2^k,$$

$$b_{111} = b_{111}(U) = w_0(U) b_{111}^0 + w_1(U) b_{111}^1 + w_2(U) b_{111}^2$$

and

$$w_i(U) = \frac{u_j u_k}{u_0 u_1 + u_0 u_2 + u_1 u_2}, \quad i \neq j \neq k$$

A collection of data $f(p_i) = f_i$ in R^3 for $i=1, \dots, n$ on the hyperbolic disc D are defined arbitrarily. In order to interpolate

this set of data, a local MQ interpolating function is extended directly to the hyperbolic disc by replacing the Euclidean distance, d_E , with the hyperbolic distance, d_H . Applying the multiquadric function to each region S_j in the hyperbolic plane, we have

$$f(p) = f_i = \sum_{i=1}^m \alpha_i B_i(d_H(p, p_i))$$

$$B_i(d_H(p, p_i)) = \sqrt{d_H(p, p_i) + R^2}$$

for $(x_i, y_i) \in S_j, i=1, \dots, m$

where m is the number of data in subdomain S_j and the hyperbolic distance d_H is defined in terms of Euclidean distance d_E ,

$$d_H(p, p_i) = \frac{1}{2} \left| \log_e \frac{d_E(pN) d_E(p_i M)}{d_E(pM) d_E(p_i N)} \right|.$$

In order to generate the multiquadric function on the hyperbolic plane, we build the linear system

$$M\mathbf{a} = \mathbf{f},$$

where

$M =$

$$\begin{bmatrix} B_1(d_H(p_1, p_1)) & B_2(d_H(p_1, p_2)) & B_3(d_H(p_1, p_3)) & \dots & B_N(d_H(p_1, p_m)) \\ B_1(d_H(p_2, p_1)) & B_2(d_H(p_2, p_2)) & B_3(d_H(p_2, p_3)) & \dots & B_N(d_H(p_2, p_m)) \\ B_1(d_H(p_3, p_1)) & B_2(d_H(p_3, p_2)) & B_3(d_H(p_3, p_3)) & \dots & B_N(d_H(p_3, p_m)) \\ \vdots & \vdots & \vdots & \ddots & \vdots \\ B_1(d_H(p_m, p_1)) & B_2(d_H(p_m, p_2)) & B_3(d_H(p_m, p_3)) & \dots & B_N(d_H(p_m, p_m)) \end{bmatrix}.$$

the unknown coefficient \mathbf{a}

$$\mathbf{a} = [a_1 \ a_2 \ a_3 \ \dots \ a_m]^T,$$

and the associated real function values

$$\mathbf{f} = [f_1 \ f_2 \ f_3 \ \dots \ f_m]^T.$$

As the number of data m is larger, the solution vector \mathbf{a} of the linear system can be obtained by using a method for the linear equation solving system such as LU decomposition method, iterative improvement of a solution to a linear equations, or singular value decomposition. Since each method provides its own advantages, choice of appropriate linear equation solving system depends on applications.

Better understanding of hyperbolic distance, the basis function of the multiquadric function on the hyperbolic plane is visualized. The geometry of the basis function B_i using the hyperbolic distance is illustrated in (Figure 4.2). The curve labeled "Euclidean distance" indicates the basis function B_i

using Euclidean distance and the one labeled “hyperbolic distance” does B , using the hyperbolic distance. Note that the similarity around the center point and the difference between them as $|x|$ increases.

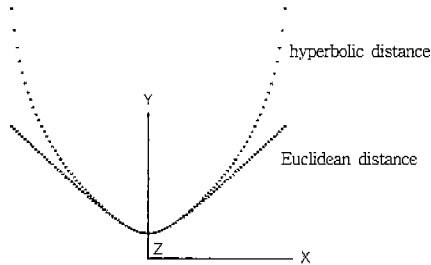


(Figure 4.2) Geometry of MQ Basis function in the hyperbolic space

For efficient implementation with the given sample data on the arbitrary triangulated domain as in (Figure 4.1), there are several initial steps for calculating the local interpolating function on the hyperbolic plane. First, generate the information on interior edge and boundary edge in the whole domain, so that their initial value can be set differently. Each triangle has its own list that contains all sample data in it and each region has the information of its member triangles. This structure makes it easier to find a region where a given data point is included.

Next stage computes the necessary coefficients for each local interpolation Q_i that interpolates the sample data points in the region S_i . The linear system of equations is solved using LU decomposition method. Once this information is set up, the final stage involves evaluating the localized interpolation $F(x, y)$ at an arbitrary point (x, y) in the domain. In order to find the triangle T_{ijk} that contains (x, y) , compute the barycentric coordinates (u_0, u_1, u_2) of (x, y) with respect to V_i, V_j , and V_k . Finally the localized interpolation can be obtained as

$$F(x, y) = W_i(x, y)Q_i(x, y) + W_j(x, y)Q_j(x, y) + W_k(x, y)Q_k(x, y)$$

4.2 Results and Comparisons

The localized MQ function on the hyperbolic disc whose radius is 1 is tested to show how it is working and to observe the difference between global and local MQ functions. For comparisons, several test functions are selected to generate the function value associated with arbitrary selected data points. With the given data points and their associate function values, global and local MQ interpolations in the

hyperbolic plane are generated and compared. The test functions are excerpted from Frankey [6], which are as follows.

$$f_1(x, y) = 0.75 \exp[-0.25(9x-2)^2 - 0.25(9y-2)^2] + 0.75 \exp\left[-\frac{(9x+1)^2}{49} - \frac{9y+1}{10}\right] + 0.5 \exp[-0.25(9x-7)^2 - 0.25(9y-3)^2] - 0.2 \exp[-(9x-4)^2 - (9y-7)^2] \tag{4.1}$$

$$f_2(x, y) = \frac{[\tanh(9y-9x) + 1]}{9} \tag{4.2}$$

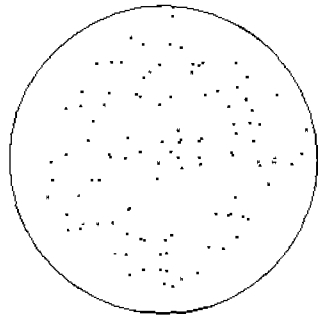
$$f_3(x, y) = \frac{1.25 + \cos(5.4y)}{6 + 6(3x-1)^2} \tag{4.3}$$

For qualitative comparisons, four arbitrary sample data sets with the number of data points n , where $n = 110, 90$, and 80 , are provided. They are shown in (Figure 4.3) (a), (Figure 4.4) (a), (Figure 4.5) (a), and (Figure 4.6) (a). Actually the data set ($n = 90$) of (Figure 4.4) (a) is obtained from the data set ($n = 110$) of (Figure 4.3) (a) by eliminating 20 data points arbitrarily. The data set ($n = 80$) in (Figure 4.5) (a) is obtained from the data set ($n = 90$) in the same way. But the data set ($n = 80$) in (Figure 4.6) (a) is another arbitrary sampled data set and is not relevant with the data sets of (Figure 4.3) thru (Figure 4.5).

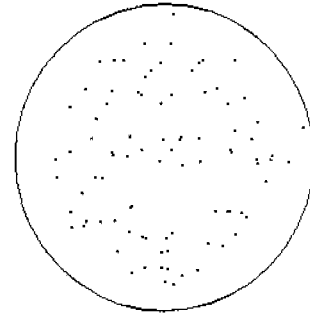
With three test functions and four sampled data sets, MQ interpolations in several aspects are tested and compared. They are global vs. local, a large data set vs. a reduced data set, and two different data sets. For comparisons between global and local interpolation, (Figure 4.3) thru (Figure 4.6) show global and local MQ interpolating functions over the arbitrary sampled data sets with $n=110, 90, 80$, and 80 respectively. Global MQ functions of using Eq. (4.1) are shown in each (b) from (Figure 4.3) thru (Figure 4.6) while local MQ functions are shown in each (c). Each (d) and each (e) show global and local MQ functions of using Eq. (4.2). Using the same method, (f) and (g) from (Figure 4.3) thru (Figure 4.6) indicate global and local MQ functions of using Eq.(4.3). In order to compare the similarity between them, the difference of function value at a certain data point is summed up and averaged. It can be written as follows.

$$avr(diff) = \sum_i^n |f_{g_i} - f_{l_i}| / n,$$

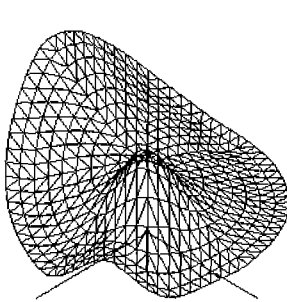
where f_{g_i} is the global interpolating function value at i^{th} data point, f_{l_i} is the local interpolating function value at the same data point, and n is the number of data points.



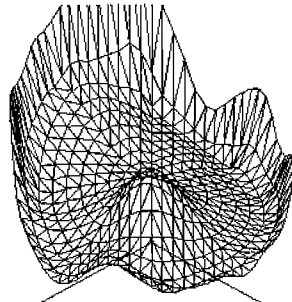
(a) Sample data ($n = 110$)



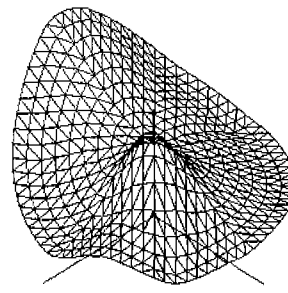
(a) Sample data ($n = 90$) obtained from (Figure 4.3) (a)



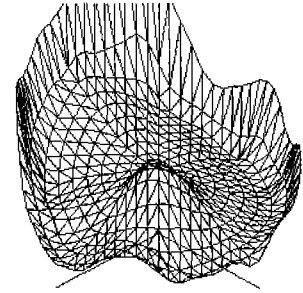
(b) Global MQ function (using Eq. (4.1))



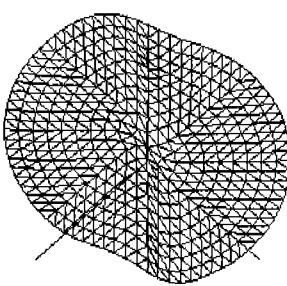
(c) Local MQ function (using Eq. (4.1))
avr(diff) between (b) and (c) is 0.009733



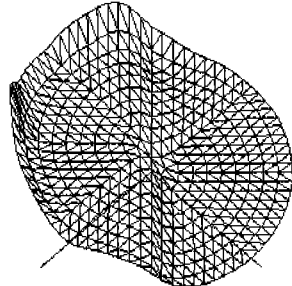
(b) Global MQ function (using Eq. (4.1))



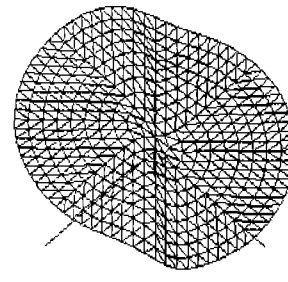
(c) Local MQ function (using Eq. (4.1))
avr(diff) between (b) and (c) is 0.013391



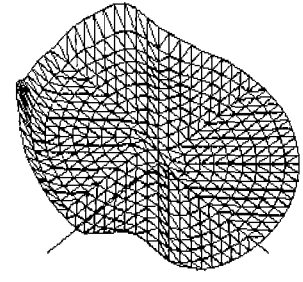
(d) Global MQ function (using Eq. (4.2))



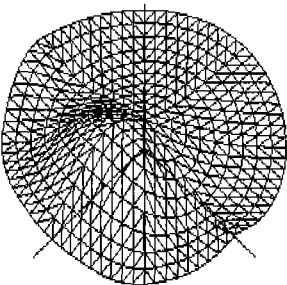
(e) Local MQ function (using Eq. (4.2))
avr(diff) between (d) and (e) is 0.003722



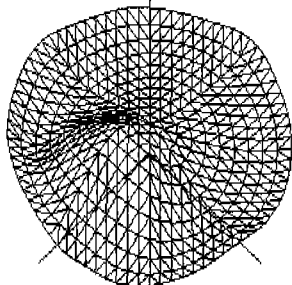
(d) Global MQ function (using Eq. (4.2))



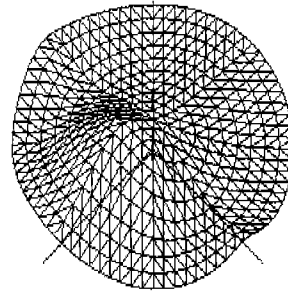
(e) Local MQ function (using Eq. (4.2))
avr(diff) between (d) and (e) is 0.003267



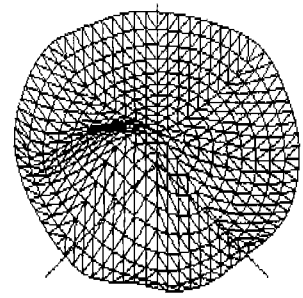
(f) Global MQ function (using Eq. (4.3))



(g) Local MQ function (using Eq. (4.3))
avr(diff) between (f) and (g) is 0.004019



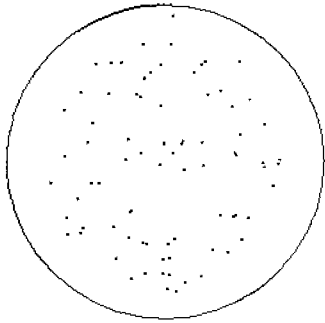
(f) Global MQ function (using Eq. (4.3))



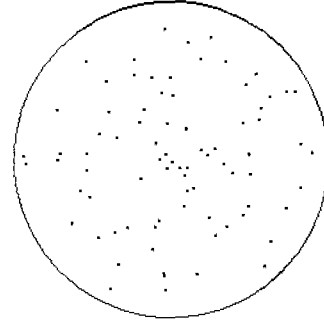
(g) Local MQ function (using Eq. (4.3))
avr(diff) between (f) and (g) is 0.003176

(Figure 4.3) Comparisons of global and local MQ functions over $n = 110$ sample data in the hyperbolic plane

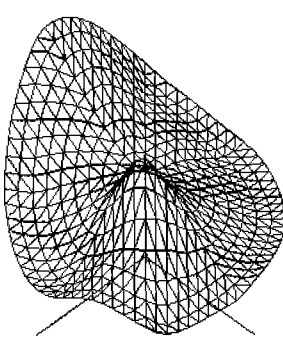
(Figure 4.4) Comparisons of global and local MQ functions over $n = 90$ sample data in the hyperbolic plane



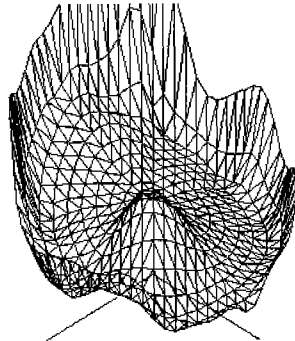
(a) Sample data ($n = 80$) obtained from (Figure 4.4) (a).



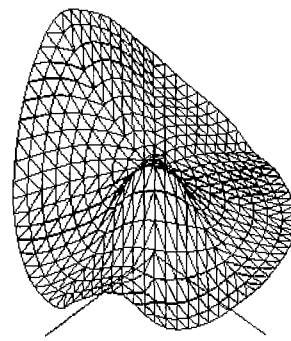
(a) Sample data ($n = 80$)



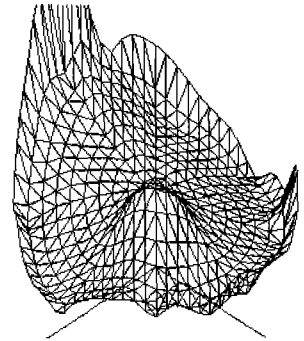
(b) Global MQ function (using Eq. (4.1))



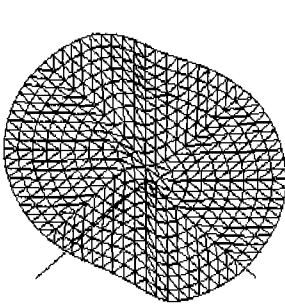
(c) Local MQ function (using Eq. (4.1))



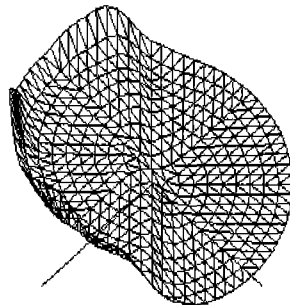
(b) Global MQ function (using Eq. (4.1))



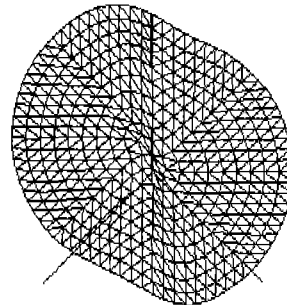
(c) Local MQ function (using Eq. (4.1)) $avr(diff) = 0.010780$



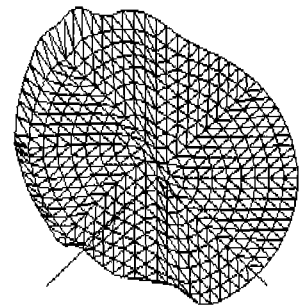
(d) Global MQ function (using Eq. (4.2))



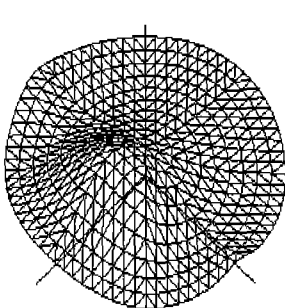
(e) Local MQ function (using Eq. (4.2))



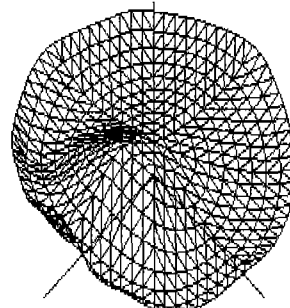
(d) Global MQ function (using Eq. (4.2))



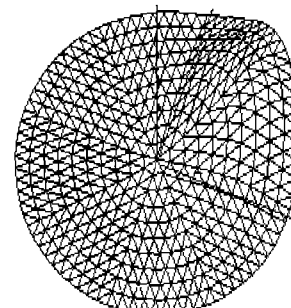
(e) Local MQ function (using Eq. (4.2)) $avr(diff) = 0.003237$



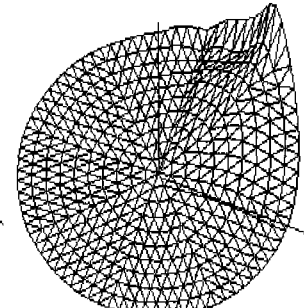
(f) Global MQ function (using Eq. (4.3))



(g) Local MQ function (using Eq. (4.3))



(f) Global MQ function (using Eq. (4.3))



(g) Local MQ function (using Eq. (4.3)) $avr(diff) = 0.002089$

(Figure 4.5) Comparisons of global and local MQ functions over $n = 80$ sample data in the hyperbolic plane

(Figure 4.6) Comparisons of global and local MQ functions over $n = 80$ sample data in the hyperbolic plane

Generally MQ interpolating functions in the hyperbolic space interpolates the given data points smoothly. As compared between global and local MQ functions, global MQ function generates stable and smooth interpolation over the overall domain while local MQ function generates stable in most of the area but increases more rapidly than global one. The result comes from the fact that the number of data points within each region in local MQ function is much smaller than that in global function. This result is very natural because the hyperbolic distance increases exponentially as it goes toward the infinity line i.e. boundary of the circle.

For comparisons, local MQ functions with a large data set vs. with a reduced data set, (Figure 4.3) thru (Figure 4.5) are utilized. The MQ interpolation using Eq. (4.1) over data set ($n = 110$) in (Figure 4.3) (c) is similar to that of data set ($n = 90$) of (Figure 4.4) (c) while it is different from that of data set ($n = 80$) of (Figure 4.5) (c). Same results are generated in the case of Eq. (4.2) and Eq. (4.3) which are depicted in (Figure 4.3) (e) thru (Figure 4.5) (e) and in (Figure 4.3) (g) thru (Figure 4.5) (g). Such results show that MQ interpolation is rougher as the data size is getting smaller. In addition, they show that local MQ interpolation is stable when the size of data set is greater than a certain number. Therefore it would be more efficient if the optimal data size would be known. However, it is difficult to find the number of optimal data size since it depends on applications.

Last, as compared between two different data sets, local MQ functions of using same functions Eq. (4.1), Eq. (4.2), and Eq. (4.3) over different data sets with $n = 80$ in (Figure 4.5) (a) and (Figure 4.6) (a), are generated and shown in (c), (e), and (g) of (Figure 4.5) and (Figure 4.6). They generate close results around central part but different at the boundary of the domain.

In conclusion, three aspects from several test functions are compared, which are global vs. local, a large data set vs. a reduced data set, and two different data sets. Even though some local MQ interpolations are looked different at the boundary of the circle, the results are generally quite satisfactory because the global and the local interpolations over fundamental domain—the polygon centered to the original point—generate very close results. Because the results between global and local interpolation are close, usage of local interpolation in the field of interactive design provides more convenient and efficient way than that of global one.

Therefore the corresponding area in the fundamental polygon will be mapped onto the object space to design a 3D genus N object. Applying local MQ interpolation into designing of genus N object is the next research work. The results and analyses on this paper can be contributed as a part of the research on interactive designing 3D genus N model. Therefore the local MQ function in the hyperbolic space provides us a strong advantage for the better way of shape control.

5. Conclusion

This research presents a new method for local interpolation of a set of scattered data on the hyperbolic disc. MQ function is localized through the process of triangulating the hyperbolic plane, evaluating the weighting functions on each region, and blending them on overlapped triangles. Over arbitrary triangle tessellation, the local MQ function in the hyperbolic plane applying the hyperbolic distance is working well and effectively. The results of this research are quite satisfactory since the shape is qualitatively recognized from the set of arbitrary scattered data. The ultimate goal of this research is to generate a local interpolation on the hyperbolic disc and eventually to make it possible to locally control a 3D object interactively over a single domain. In terms of this view, the result is considered to be the first step toward the goal.

As the future works, this method will be utilized to design a 3D object with infinite continuity over a single domain, which will provide a more efficient design method. On the other hand, a subdivision scheme should be integrated into the design of an object. Therefore, further study is needed for finding a full subdivision on the hyperbolic disc.

References

- [1] R. E. Barnhill, "Surfaces in Computer aided geometric design : A survey with new results," *Computer Aided Geometric Design* 2, pp.1-17, 1985.
- [2] G. Farin, *Curves ad Surfaces in Computer Aided Geometric Design 4th*, Academic Press, Boston, 1996.
- [3] H. Ferguson, A. Rockwood, J. Cox, "Topological design of sculptured surfaces," *Computer Graphics* 26(3), pp.149-156, 1992.
- [4] H. Ferguson, A. Rockwood, "Multiperiodic functions for surface design," *Computer Aided Geometric Design* 10,

pp.315-328, 1993.

[5] P. Firby, C. Gardiner, *Surface Topology*, Wiley, New York, 1982.

[6] R. Franke, "Scattered data Interpolation : Tests of some methods," *Mathematics of Computation* 38, pp.181-200, 1982.

[7] R. Franke, "Smooth interpolation of scattered data by local thin plate splines," *Computer and Mathematics with Applications* 8, pp.273-281, 1982.

[8] R. Franke, G. M. Nielson, "Scattered data interpolation and application : A tutorial and Survey," in Hagen, H., Roller, D. (ed.), *Geometric Modeling*, Springer, pp.131-160, 1991.

[9] R. L. Hardy, "Multiquadric equations of topography and other irregular surfaces," *Journal Geophysical Research*, 76, pp.1905-1915, 1971.

[10] R. L. Hardy, "Theory and Applications of the multiquadric biharmonic method," *Computers and Mathematics with Applications* 19, pp.163-208, 1990.

[11] J. Hoschek, D. Lasser, *Fundamental of Computer Aided Geometric Design*, AK Peters, Wellesley, Massachusetts, 1993.

[12] B. Iversen, *Hyperbolic Geometry*, Cambridge University Press, Cambridge, 1992.

[13] J. G. Ratcliffe, *Foundations of Hyperbolic manifolds*, Graduate Texts in Mathematics 149, Springer Verlag, 1994.

[14] A. Rockwood, H. Park, "Interactive Design of Smooth Genus N Objects using Multiperiodic Functions and Applica-

tions," *International Journal of shape modeling*, Vol.5, No.2, pp.135-157, 1999.

[15] T. A. Foley, S. Dayanand and D. Zeckzer, "Localized radial basis methods using rational triangle patches," *Computing*, Vol.10, pp.163-176, 1995.

[16] J. Duchon, "Splines minimizing rotation-invariant seminorms in Sobolev spaces," In *Constructive Theory of Functions of Several Variables*, (Edited by W. Schempp and K. Zeller), *Lecture Notes in Mathematics* 571, Springer, New York, pp.85-100, 1977.



박 화 진

e-mail : hwajinpk@sookmyung.ac.kr

1987년 숙명여자대학교 전산학과 졸업
(학사)

1989년 숙명여자대학교 대학원 전산학과
졸업 (석사)

1997년 Arizona State University Dept.
of Computer Science 컴퓨터
그래픽 전공(공학박사)

1997년~1998년 삼성 SDS 연구소 선임연구원

1998년~2000년 평택대학교 전임강사

2000년~현재 숙명여자대학교 정보과학부 멀티미디어학전공
조교수

관심분야 : 컴퓨터 그래픽, 3D 모델링, 가상현실, 멀티미디어